Journal of Power Sources 182 (2008) 223–229

Contents lists available at ScienceDirect

Journal of Power Sources

journal homepage: www.elsevier.com/locate/jpowsour

Hygrothermal effects on properties of highly conductive epoxy/graphite composites for applications as bipolar plates

Ling Du, Sadhan C. Jana*

Department of Polymer Engineering, University of Akron, 250 South Forge Street, Akron, OH 44325-0301, United States

ARTICLE INFO

Article history:
Received 27 January 2008
Received in revised form 18 March 2008
Accepted 19 March 2008
Available online 3 April 2008

Keywords:
Graphite/epoxy composite
Hygrothermal effects
Water diffusion mechanism
Polymer composite bipolar plates

ABSTRACT

The hygrothermal effects on mechanical, thermal, and electrical properties of highly conductive graphite-based epoxy composites were investigated. The highly conductive graphite-based epoxy composites were found to be suitable for applications as bipolar plates in proton exchange membrane (PEM) fuel cells. The hygrothermal aging experiments were designed to simulate the service conditions in PEM fuel cells. Specifically, the composite specimens were immersed in boiling water, aqueous sulphuric acid solution, and aqueous solution of hydrogen peroxide. The water uptake, changes in surface appearance and dimensions, glass transition behavior and thermal stability, and electrical and mechanical properties were evaluated. The water uptake at short time increased linearly with the square root of time as in linear Fickian diffusion. The presence of graphite significantly reduced both the rate and extent of water uptake. No discernible changes in specimen dimensions, surface appearance, and morphology of the composites were observed. The electrical conductivity and mechanical properties remained almost unchanged. The wet specimens showed slight reduction of glass transition temperature (T_g) due to plasticization of epoxy networks by absorbed water, while the re-dried specimens showed small increase of T_g. The composites maintained high electrical conductivity of about 300–500 S cm^{-1} and good mechanical properties and showed thermal stability up to 350 °C.

© 2008 Elsevier B.V. All rights reserved.

1. Introduction

Proton exchange membrane (PEM) fuel cells are considered one of the most promising environmentally friendly power sources for various electronic devices, and transportation and stationary applications [1–5]. An integral part of PEM fuel cells is bipolar plates which performs multiple functions and has become the subject of recent extensive research [6–26]. Conventional pure graphite bipolar plates contribute significantly to the cost and weight of PEM fuel cell stacks. Metals such as stainless steel and metal alloys – alternatives favored by industry – are not preferable because of corrosion-related issues [8,9], although coatings by carbon film [10], polypyrrole [11], gold [12], and chromium nitrides [13] have been found useful. In view of this, the development of lightweight, low cost and highly conductive polymer composite bipolar plates with scope for mass production can enable rapid commercialization of PEM fuel cells [3,5,14,15]. Recent literature shows significant progress in graphite-based composite bipolar plates with useful attributes as light-weight, low cost, and desired properties [25]. Polymer composite bipolar plates are now commercially available from commercial suppliers such as DuPont, H2 Economy, ICM Plastics, NedStack, to name a few. This shows that the technology of polymer composite bipolar plates is rapidly maturing. Nevertheless, many challenges still exist. For example, PEM fuel cells are operated at temperatures greater than 80 °C and under high humidity and highly acidic environment. Consequently, bipolar plates are exposed to high temperatures, high humidity, and highly acidic membranes and gaseous oxygen over a long period of time. In view of this, it is critical to evaluate the combined effects of these severe PEM fuel cell in-service conditions on the properties of potential polymer composite bipolar plates. A very limited literature exists on investigation of hygrothermal reliability and durability of polymer composite bipolar plates at the PEM fuel cell service conditions. In view of this, we undertook a study in our laboratory on hygrothermal aging of polymer composite bipolar plates with specific emphasis on expanded graphite (EG)–epoxy composites.

In an earlier study [26], we reported the development of epoxy-based polymer composites suitable as bipolar plates with high electrical conductivity and glass transition temperatures greater than 150 °C. In addition, strong mechanical properties, good thermal and chemical properties, and good gas tightness at dry states

* Corresponding author. Tel.: +1 330 972 8293; fax: +1 330 258 2339.
E-mail address: janas@uakron.edu (S.C. Jana).

0378-7753/$ – see front matter © 2008 Elsevier B.V. All rights reserved.
doi:10.1016/j.jpowsour.2008.03.071

were reported. It is imperative that the polymer composites bipolar plates should also exhibit long-term resistance to hygrothermal aging fatigue, chemical corrosion, and thermal degradation under PEM fuel cell service conditions in order to be viable for economically successful PEM fuel cells.

It is learned from existing literature that hygrothermal aging is a degradation process that combines the effects of moisture and temperature and results in substantial deterioration of the thermal and mechanical properties of polymers and polymer composites. A large number of studies reported the effects of hygrothermal aging on polymers and fiber-reinforced polymer composite laminates [27–62]. Some researchers suggested multiple water diffusion mechanisms, ranging from the simplest case, a Fickian model, where diffusion is driven by the water concentration gradient, to the more complex stress-dependent, history-dependent, and dual-phase diffusion models. Although Fickian diffusion is often assumed, diffusion in thermosetting polymers usually involves the concentration-gradient-driven Fickian diffusion, and a time-dependent relaxation process. This results in phased or pseudo-Fickian response, usually called the two-stage diffusion model [38]. Fickian diffusion behavior is observed when no chemical degradation occurs in materials [42,47,55,59]. Thus, Fickian diffusion may indirectly indicate that the hygrothermal effects are reversible. Non-Fickian diffusion behavior, on the other hand, usually relates to either chemical degradation of the materials or matrix cracking, and interface debonding between the fillers and the polymers [36,41,46,49,52,55–57].

Hygrothermal exposure of polymers and composites can often lead to significant drop in glass transition temperature (T_g) of the materials [37,38,41,46–48,50,52,54,58,61,62]. Such drop in T_g can sometimes be more than 50 °C as reported by Cornelia [61,62] for the bismaleimide (BMI)- and polyimide (PI)-carbon fiber composites, and in some rare cases can be as high as 100 °C. Mechanical properties, such as tensile modulus and tensile strength, flexural modulus and strength, and adhesion strength also show significant deterioration [27,30–35,39–40,42,43,45,46,51,58,60]. For example, Ishak et al. [42] reported a reduction of tensile properties for short glass fiber-reinforced poly(butyleneterephthalate) composites. A number of other researchers also reported either no change or a slight increase in mechanical properties after hygrothermal exposure [30,37,39,40,51]. Long-term hygrothermal exposure can also cause matrix swelling and cracking, moisture vapor-induced microvoids, interface debonding behavior between fillers and matrix, surface blistering, and microstructural and composition change due to chemical degradation, such as oxidation and hydrolysis [28–35,43,45,53–58]. These detrimental changes will eventually cause damage to the materials and hence failure of the components.

A ramification of reduction in wet T_g, can be microvoids and surface blistering. For example, if the wet T_g approaches the fuel cell operating temperature, the internal vapor pressures due to moisture can be sufficiently high and can generate both interior microvoids and small surface blistering. This is aided by accelerated polymer relaxation at temperatures higher than the wet T_g. In addition, the intrinsic properties of the polymers and the composites, such as mechanical properties, can significantly deteriorate. Consequently, the values of wet T_g set the acceptable upper limit of the service temperature. Thus, water diffusion behavior in polymer composite bipolar plates plays a crucial role in determining the wet T_g and hence the performance towards microvoid generation and mechanical failure.

In view of the importance of wet T_g, it is useful to fully understand the mechanism of water diffusion in polymer composites. In addition, the effects of the PEM fuel cell service conditions on the properties of the polymer composite bipolar plates must be studied before they can be confidently used in PEM fuel cells. This paper investigated water diffusion mechanism, hygrothermal aging effects on the thermal, chemical, mechanical, and electrical properties of epoxy resins, and graphite/epoxy composites.

2. Experimental

2.1. Materials

The composite materials were synthesized from a mixture of an aromatic and an aliphatic epoxy resin, the rationale for which was provided in our earlier work [26]. The aromatic epoxy was diglycidyl ether of bisphenol A in the form of Epon® 826, obtained from Resolution Performance Products (Houston, TX) with epoxide equivalent weight of 178–186, viscosity of 65–95 Pa s, and specific gravity of 1.15 at 25 °C. The aliphatic epoxy was polypropyleneglycol glycidyl ether in the form of Araldite® DY3601, received from Vantico (Brewster, NY) with epoxide equivalent weight of 385–405, viscosity of 0.42–0.52 Pa s, and specific gravity of 1.03 at 25 °C. The curing agent, diaminodiphenylsulphone (DDS) was received from Ciba (Tarrytown, NY) with trade name HT976, melting temperature 180 °C and molecular weight 248 g mol^{-1}. Epon® 826 cured with DDS produced a brittle material, while Araldite® DY3601 cured with DDS produced a gum-like material. In view of this, we resorted to a mixture of 90:10 (wt%) of Epon® 826 and Araldite® DY3601, which yielded more ductile material when cured with DDS. The material will be referred to in the rest of the paper as EP90. Electrically conductive carbon black (CB), Ketjenblack® EC-600JD was received from Akzo Nobel Chemicals Inc. (Chicago, IL). Expandable graphite (EG), GRAFGUARD® Expandable Flake 160-50N with high expansion volume of ~250 cm^3 g^{-1} at 600 °C was obtained from GrafTech (Cleveland, OH). Mixtures of EG and CB were used to make composites electrically conductive.

2.2. Preparation and characterization of composites

Epoxy resin mixture was prepared by mixing Epon® 826 and Araldite® DY3601 at the weight ratio of 90:10 in a beaker at room temperature, followed by addition of 5 wt% excess curing agent DDS than necessary to balance the stoichiometry of epoxide and amine groups. Clear solutions were obtained by heating the mixtures up to 135 °C with stirring. Alternatively, the epoxy-curing agent mixture was prepared by mixing all three components in a beaker with acetone as the solvent. Electrically conductive composites were prepared by solution intercalation method, whereby desired quantities of EG and CB were added to the solution of epoxy resins and curing agent in acetone. Accordingly, the composites are designated in the rest of the paper by the parts by weight of epoxy, EG, and CB; for example, the composite 50–45–5 contained 50 parts by weight of epoxy, 45 parts by weight of EG, and 5 parts by weight of CB. The materials were mechanically stirred for 6 h, after which the solvent was allowed to evaporate at room temperature with continuous stirring. The remaining trace of acetone was removed by drying in a vacuum oven for 24 h at 60 °C, and 2 h at 110 °C. The dried materials were obtained in powder form and were compression molded into composite sheets at a pressure of 4000 psi and cured at 180 °C for 4–6 h, followed by post-curing in vacuum oven at 200 °C for 6 h.

Specimens for evaluation of hygrothermal effects were cut from the compression molded sheets. The thickness of the specimen was approximately 0.5 mm. This guaranteed one-dimensional diffusion of water perpendicular to the specimen surface. A typical specimen had the following dimensions: 80 mm × 10 mm × 0.5 mm. The specimens of cured epoxy resins and composites were immersed in boiling water, boiling aqueous solution of sulphuric acid (pH 1–2),

and boiling aqueous solution of 6 wt% hydrogen peroxide and kept for a period of up to 6 months under continuous reflux. The pH of the acid solution was periodically checked and adjusted to 1–2. The specimens were periodically withdrawn from the reflux apparatus, dried using lint-free tissues to remove the surface liquid, and weighed. The electrical conductivity was also measured. Finally, the specimens were dried in a high vacuum oven for 3 months at 60 °C, and for an additional 3 months at 140 °C. The glass transition and thermal degradation temperatures of wet and dry specimens were measured. The elastic (G') and loss (G'') modulus of the epoxy resins and composites were measured by dynamic mechanical analysis (DMA) after the hygrothermal aging process. Note that elastic and loss modulus relate to the viscoelastic response of the materials when subjected to sinusoidal strain. The ratio $\tan\delta \equiv G''/G'$ is referred to as the loss tangent. The plots of $\tan\delta$ vs. temperature were used to infer glass transition temperature of cured epoxy and composites. Dynamic mechanical analysis was performed with a Pyris Diamond DMA, from PerkinElmer-Seiko Instruments (Boston, MA) in tensile mode at 3 °C min^{-1} under nitrogen atmosphere, 1 Hz frequency, and thermal scans from room temperature (25 °C) to 300 °C. Thermal stability of composites was investigated in a TGA 2050 device from TA Instruments (New Castle, DE). Specimens weighing ca. 6 mg were subjected to thermal scan from room temperature up to 1000 °C, at a scan rate of 20 °C min^{-1} in nitrogen gas. The changes in morphology of the specimens due to hygrothermal exposure were inspected by scanning electron microscopy (SEM). The specimens were dipped in liquid nitrogen and fractured by impact. The fractured samples were coated with silver using a K575x sputter coater from Emitech (Kent, England) under argon gas atmosphere. Surface morphology was observed using a SEM S-2150 from Hitachi (Ibaraki, Japan) at 25 kV.

3. Results and discussion

The data on hygrothermal aging in acid solution and in water are discussed below. It was found that the surface appearance, electrical conductivity, and dynamic mechanical properties of specimens subjected to hygrothermal aging in 6 wt% hydrogen peroxide solution were indistinguishable from those in water. In view of this, the data on hygrothermal exposure in hydrogen peroxide solution are not discussed.

3.1. Water absorption

The mechanism of water diffusion was studied from the amount of water uptake by the specimens. The water uptake was calculated from Eq. (1):

$$M(\%) = \frac{W - W_d}{W_d} \times 100 \quad (1)$$

In Eq. (1), M is water uptake in percent by weight of the dry specimen, W is the weight of the specimen at time t, and W_d is the weight of the dry specimen. Water absorption profiles for the epoxy resin and composites are presented in Fig. 1. It is apparent that the water absorption in all materials followed the Fickian diffusion model, whereby the amount of absorbed water increased linearly with the square root of time in the early periods and reached equilibrium water content after about 100 h. This is contrary to what was observed by other researchers, e.g., Zhou and Lucas [46] reported non-Fickian water diffusion behavior in graphite/epoxy composite laminates at reflux temperature greater than 90 °C. Bao et al. [36,55–57] reported two-stage diffusion model for the bismaleimide matrix carbon fiber composites system with the first and the second stages being diffusion- and relaxation-controlled, respectively. It is seen from Fig. 1 that the maximum water uptake

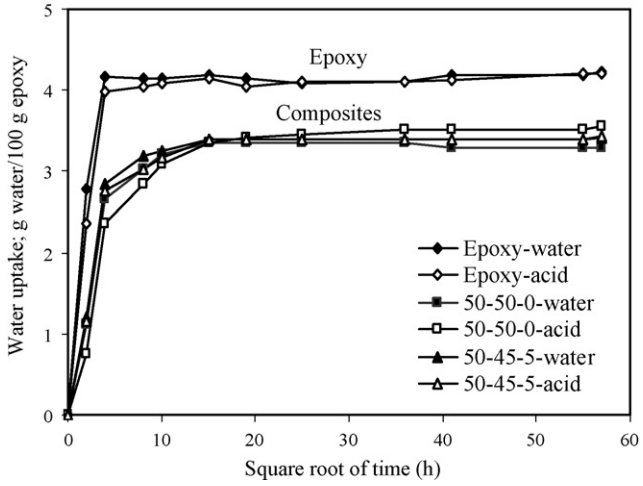

Fig. 1. Water uptake with time by cured epoxy and epoxy composites of EG and CB. Water uptake is given as gram of water per one hundred gram of cured epoxy.

by neat cured epoxy was 4.3 g water per 100 g cured epoxy. The composites, on the other hand, showed substantial reduction in water uptake, e.g., about 3.4 g water per 100 g cured epoxy, which was equivalent to 1.8 g water per 100 g of cured composite. Such reduction in total water absorption in composites can be attributed to the presence of EG and CB fillers. The presence of close to 50 wt% of EG should also make the composites more hydrophobic in nature. A positive ramification of this can be easier water management in the operation of fuel cells.

Although water absorption profiles in Fig. 1 present a clear trend, it is interesting to determine and compare the values of water diffusivity in the epoxy resin and composites. Water diffusivity, D, in epoxy resins and composites were calculated from the initial slope of the water absorption profiles shown in Fig. 1 and Eq. (2) [47]. Such data is presented in Table 1.

$$D = \frac{\pi}{16}\left(\frac{h}{M_m}\right)^2 \left(\frac{M_{t_2} - M_{t_1}}{\sqrt{t_2} - \sqrt{t_1}}\right)^2 \quad (2)$$

where h is the thickness of the specimen, M_m is the maximum water uptake of the specimen, M_{t_1} and M_{t_2} are the weights of the specimen at times t_1 and t_2, respectively. The values of times t_1 and t_2 were chosen in the linear regime in Fig. 1. A clear trend is apparent from the data in Table 1. Water diffusivity of composites was more than an order of magnitude smaller than those of epoxy resins. This can be attributed to the hydrophobic nature and the layered structure of EG particles which presented higher barrier to diffusion of water molecules.

Table 1
Water diffusivity in epoxy resin and composites

Material Epoxy/EG/CB	Medium	M_m (%) (6 months)	D ($\times 10^{-6}$ mm^2 s^{-1})
100/0/0	Water	4.22	8.4
100/0/0	Acid	4.20	10.2
50/50/0	Water	1.62	0.46
50/50/0	Acid	1.59	0.34
50/47/3	Water	1.77	0.53
50/47/3	Acid	1.72	0.52
50/45/5	Water	1.46	0.69
50/45/5	Acid	1.52	0.66

The materials are designed by parts by weight of epoxy, EG, and CB.

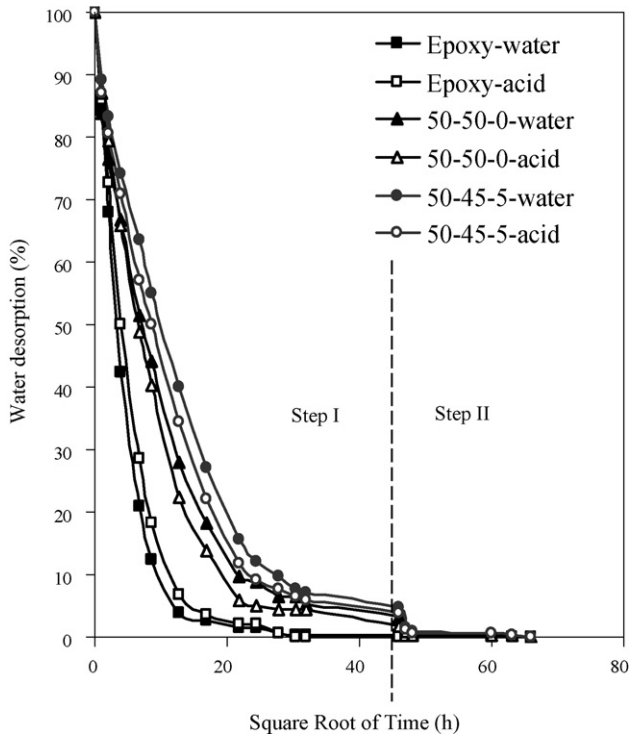

Fig. 2. Water desorption profile of epoxy resin and composites during drying after hygrothermal exposure. The drying temperature in Steps I and II were, respectively, 60° and 140 °C. In this case, 100% absorbed water for each composite represent the value of M_m in Table 1.

3.2. Water desorption profile

Water desorption profile was obtained by drying the specimens at 60 °C for 3 months, referred to as Step I, and then at 140 °C for another 3 months, referred to as Step II. The weight percent of moisture remaining in specimens in various steps is shown in Fig. 2. The amount of water desorbed was calculated from Eq. (3):

$$M_{loss}(\%) = \frac{M_m - M_t}{M_m} \times 100 \quad (3)$$

$$M_t = W_t - W_d \quad (4)$$

where the M_{loss} is the percentage of weight loss due to desorption of water, M_m is the maximum water uptake by the specimens obtained from the data in Fig. 1, M_t is the weight of water that remained in the specimens at time t, W_t is the weight of the specimens at time t, and W_d is the weight of the dry specimens. Fig. 2 reveals that the weight of desorbed water also showed linear behavior with the square root of time at the beginning, and reached a plateau at long time at the drying temperature of 60 °C (Step I). Note however, that not all water absorbed by the sample could be removed in Step I, e.g., approximately 4 wt% of the original absorbed water (M_m in Table 1) could not be removed from the specimens with further increase of drying time at 60 °C. This residual water in the specimens is referred to as locked-in water [47] and can only be removed at temperatures higher than the boiling temperature of water. In view of this, the drying temperature was elevated to 140 °C in Step II. Zhou and Lucas [47] postulated that two types of bound water exist for cross-linked epoxy resins. Type I water (as in Step I) is bound by Van der Waals forces or by single hydrogen bonding, while the residual water molecules (removed in Step II) are usually multiply hydrogen bonded with the epoxy molecules and are termed Type II bound water. Thus the trend seen in Fig. 2 reveals that both Type I and Type II bound water were present in the materials considered in this work.

The water that was removed at 60 °C may have resided in the free volume of the samples or was bound with epoxy molecules by Van der Waals and/or single hydrogen bonding. Fig. 2 reveals that this Type I bound water was easily removed from the samples and constituted the majority of water absorbed in the samples. It is seen in Fig. 2 that the original weights of the specimens were recovered after drying at temperature of 140 °C for 3 months. This indicates that water absorption–desorption process is reversible, a ramification of which is the absence of chemical degradation during the reflux process, such as hydrolysis of epoxy. However, some researchers reported weight loss after hygrothermal aging process, indicating the possibility of chemical degradation [28–35,43,45,53–58], which was not the case in this study.

Fig. 2 also reveals that the water desorption rate of graphite/epoxy composites was much lower than that of unfilled epoxy resin. Thus, it can be inferred that EG particles not only slowed down the water absorption rate as seen in Fig. 1, but also slowed down the water desorption rate. Note that both water absorption and desorption processes are governed by water diffusion and that the presence of EG particles in the composites substantially reduced the value of water diffusion coefficient (Table 1). After the drying Step I, the epoxy resin recovered most of its original weight, but some locked-in water remained in all graphite/epoxy composites. The locked-in water was finally removed from the samples in Step II. As will be seen later, this behavior affected the value of thermal degradation temperature T_1.

3.3. Dimensional stability, surface appearance, and morphology

The specimens subjected to water and acid reflux presented no discernible changes in material dimensions. The thickness of the specimens recorded before and after reflux and after drying did not show any change from the original specimen thickness, indicating that the specimens had excellent dimensional stability. An inspection by optical microscope also did not reveal any changes in surface appearance in specimens.

Some researchers reported that hygrothermal aging processes caused micro-cracking, micro-voids, or debonding at the interface between fillers and polymer matrices caused by water [29,44]. The morphology of cold-fractured surfaces of composite specimens after hygrothermal exposure was inspected by scanning electron microscopy as presented in Fig. 3. The SEM images presented in Fig. 3 show no apparent interface debonding between graphite particles and epoxy and no micro-cracking or micro-voids in the composites. The absence of interface debonding between graphite and epoxy can be interpreted as follows. Graphite layers are known to contain the functional groups, such as carboxyl, epoxide, hydroxyl, and carbonyl on the surface [63–66], as revealed from X-ray photoelectron spectroscopy (XPS) data presented in Figs. 4 and 5. The XPS data was obtained using a VG ESCALAB Mk II system under high vacuum conditions. The aluminum anode on a Mg/Al X-ray source was used at a power of 180 W with a fixed analyzer transmission energy of 100 eV. Specifically, Fig. 5 presents evidence that the EG particles used in this work contained carboxyl, carbonyl, ether, epoxide, and ester functional groups contributing to approximately 3.9 wt% of the surface composition. Of these, carboxyl and epoxide can react with the amine groups of the curing agent DDS and result in covalent bonding between graphite and epoxy. In addition,

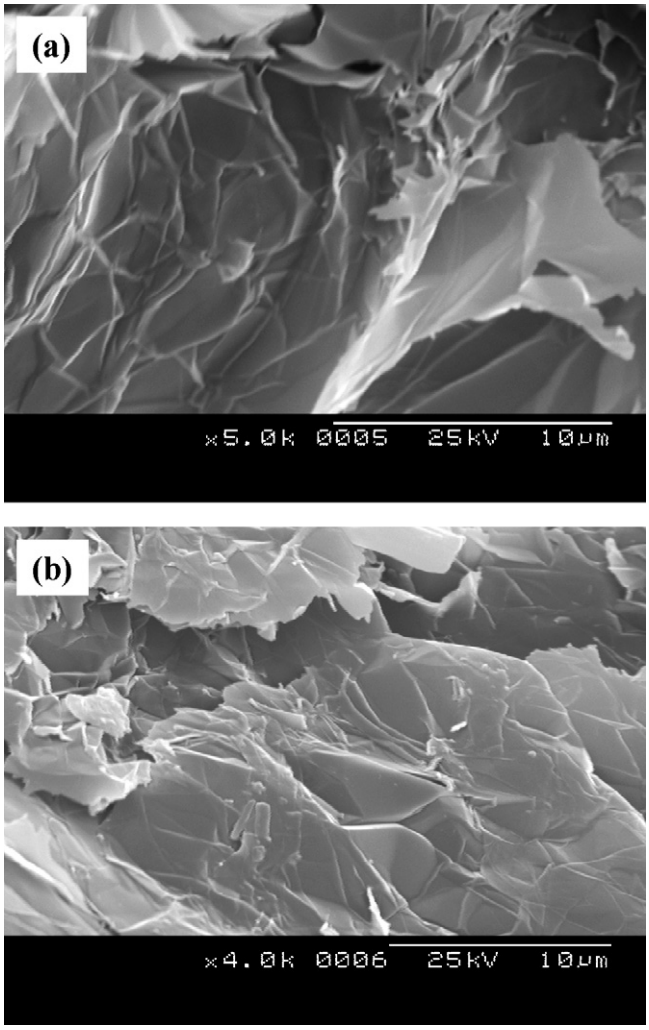

Fig. 3. Morphology of cold fractured specimen EP/EG/CB (50/50/0) composite (a) before and (b) after hygrothermal exposure in acid solution obtained by scanning electron microscopy method.

the polar functional groups on graphite particles also participate in hydrogen bonding with hydroxyl and substituted amine groups in cross-linked epoxy. The strongly bonded interface thus formed delivers high resistance to water attack on the interfaces.

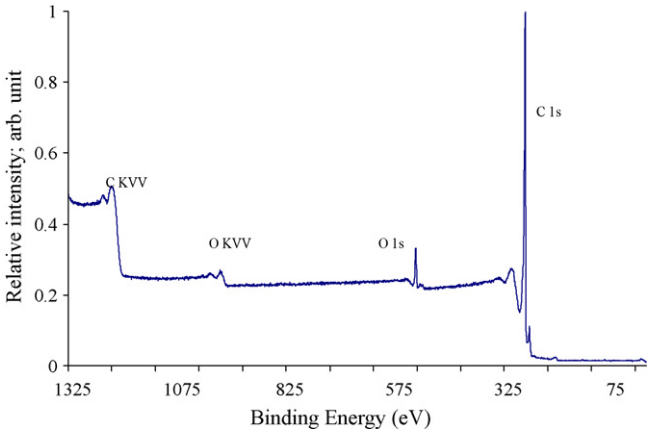

Fig. 4. XPS spectrum of expanded graphite.

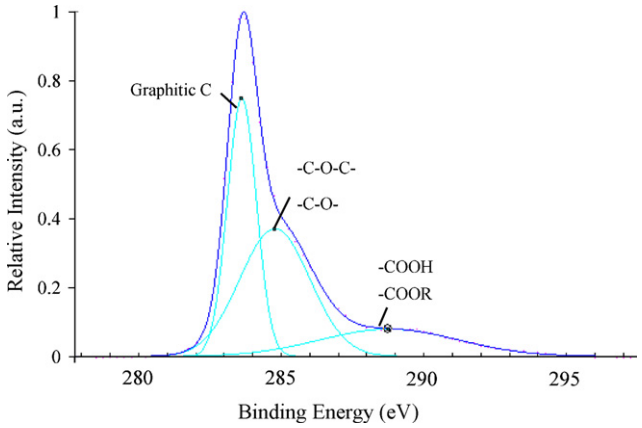

Fig. 5. Narrow XPS spectrum of the C (1s) region of EG. The convoluted peaks corresponding to graphitic carbon and polar functional groups are shown.

3.4. Electrical conductivity and mechanical properties

It is imperative that the graphite/epoxy composites must have very high electrical conductivity at the dry state and should maintain high electrical conductivity during the service life. Thus one aim of this study was to monitor the electrical conductivity of the composites during the hygrothermal exposure. The electrical conductivity of the epoxy composites was measured periodically during the hygrothermal aging process, and the data is shown in Fig. 6. It is seen that electrical conductivity of the specimens decreased only slightly due to hygrothermal exposure, and all specimens maintained electrical conductivity at higher than 400 S cm^{-1}. Note that the conductive filler content in these composites was substantially higher than the percolation threshold. Thus, water uptake had very little influence on the global conductive filler network structures in these composites. In view of the data presented in Fig. 6, we can infer that the composites studied in this work should be able to maintain stable high values of electrical conductivity at the PEM fuel cell service conditions.

The polymer composite bipolar plates should also retain good mechanical properties so as to support thin membranes and electrodes, and withstand the clamping forces for the PEM fuel cell stack assembly. Thus hygrothermal effects on mechanical properties of epoxy resin and composites also need to be monitored. In this paper, the mechanical properties were inferred from dynamic mechanical properties of the materials after hygrothermal exposure. A set of representative data is presented in Fig. 7.

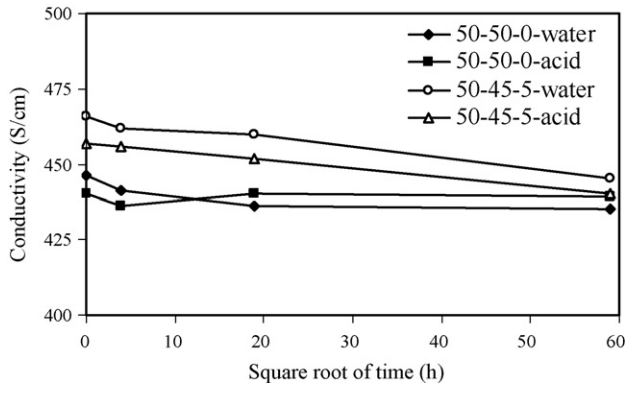

Fig. 6. Change in in-plane electrical conductivity of composites with time of hygrothermal exposure. Solid lines connect data points and guide the eye.

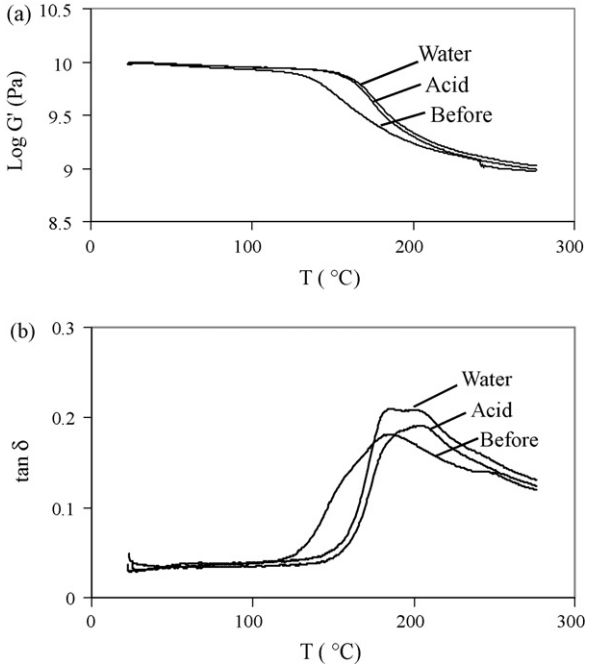

Fig. 7. Effect of hygrothermal exposure on (a) storage modulus (G') and (b) loss tangent ($\tan\delta$) of EP/EG/CB (50/45/5) composite obtained by DMA. Data obtained prior to hygrothermal exposure are designated as "Before".

Table 2
Glass transition temperatures inferred from the peaks of $\tan\delta$ vs. temperature curves of DMA before and after hygrothermal aging process

Epoxy/EG/CB	T_g (°C)		
	Before	Water	Acid
100/0/0	186	185	189
50/50/0	190	204	203
50/49/1	188	204	202
50/48/2	187	205	204
50/47/3	189	201	202
50/46/4	185	203	202
50/45/5	189	202	201
50/44/6	186	202	201

It is seen from Fig. 7 that the values of storage modulus (G') increased due to hygrothermal exposure, which is counter-intuitive. It is also seen that the materials subjected to hygrothermal exposure maintained high values of G' up to approximately 160 °C compared to 130 °C in the case of the original materials. This also indicates that no degradation occurred in the materials as already discussed. The loss tangent ($\tan\delta$) vs. temperature plots of composites show that the peaks of $\tan\delta$ shifted to higher temperatures for all composites after reflux, indicating that the glass transition temperatures also increased as a result of the hygrothermal exposure. Table 2 presents the values of T_g determined from the peak of $\tan\delta$ vs. temperature plots as function of the type and the amounts of fillers. The trend presented in Table 2 was also verified from measurement of T_g by differential scanning calorimetry (DSC), see Table 3. A TA Instruments (New Castle, DE) DSC 2920 Modulated DSC was used for this purpose with a heating rate of 10 °C min^{-1}. Another curious observation can be made from the data presented in Fig. 7b; the peaks of $\tan\delta$ for composites became very broad and even split into two peaks after hygrothermal exposure. This kind of splitting of the peaks of $\tan\delta$ was observed earlier by other researchers [38,44] and can be attributed in our case to slow post-curing that occurred during long-term (6 months) exposure of the

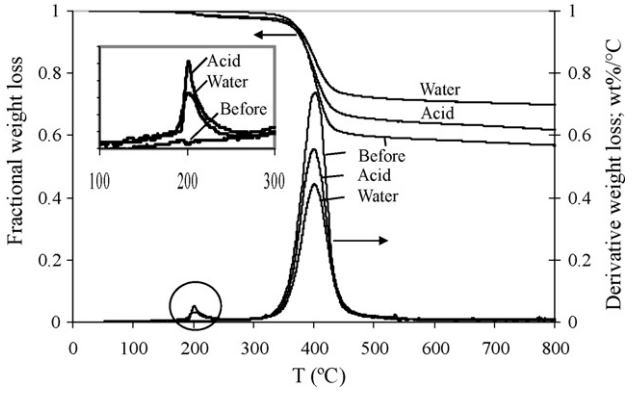

Fig. 8. Thermal degradation temperatures of EP/EG/CB (50/45/5) composites before and after hygrothermal exposure determined by TGA.

specimens to boiling water and boiling acid solution. The same argument of long-term post-curing can be invoked to interpret the increase of storage modulus in materials subjected to hygrothermal exposure (Fig. 7a). The unfilled, cured epoxy also showed an increase of the values of storage modulus upon hygrothermal exposure. The same observation was made by other researchers in the case of phenol novolac epoxy cured by DDS [67].

3.5. Thermal stability of the composites

The thermal stability of the composites was characterized in terms of thermal degradation temperatures (T_1 and T_2), derived from fractional weight loss vs. temperature plots. A representative plot is shown in Fig. 8. In this case, T_1 and T_2 represent the temperature at 5 wt% weight loss and the maximum rate of weight loss, respectively. The values of T_g measured by DSC, T_1, and T_2 of composites are presented in Table 3. It is evident that T_g of wet specimens decreased slightly. However, after re-drying, the values of T_g were restored to their values before hygrothermal exposure. A slight increase is also seen for some re-dried specimens. The reduction in T_g of wet specimens can be attributed to the moisture-induced plasticization, while the increase in T_g of the re-dried specimens was due to post-curing of epoxy. Some researchers suggested that loss of small molecules during long-term hygrothermal exposure may also cause an increase in T_g [38,68]. In our case, however, the water desorption data in Fig. 2 indicate that this

Table 3
Glass transition temperatures determined by DSC (scan rate 10 °C min^{-1}) and thermal degradation temperatures of epoxy resin and composites before and after hygrothermal aging process

Material	Conditions	T_g (°C)	T_1 (°C)	T_2 (°C)
Epoxy	Before	182	390	424
	Wet water	171	367	424
	Wet acid	172	352	424
	Re-dried water	187	NA	NA
	Re-dried acid	186	NA	NA
50/50/0	Before	177	392	415
	Wet water	170	371	416
	Wet acid	169	305	413
	Re-dried water	182	NA	NA
	Re-dried acid	181	NA	NA
50/45/5	Before	174	370	402
	Wet water	168	363	393
	Wet acid	167	358	395
	Re-dried water	179	NA	NA
	Re-dried acid	180	NA	NA

was possibly not true and that there was no dissolution loss from the epoxy resin and the composites. Thus, the increase in T_g seen in Tables 2 and 3 should be attributed to the post-curing of the specimens during hygrothermal exposure. For wet samples with absorbed water, however, the plasticization effect dominated over the effect of post-curing and caused an overall reduction in T_g.

The data in Table 3 shows that after water and acid refluxes, T_2 remained at the same high values as for materials before reflux. The values of T_1 of specimens decreased after reflux owing to water evaporation upon heating. The small peaks in the derivative of weight loss data for all graphite/epoxy composites correspond to to the removal of water at around 200 °C. The inset of Fig. 8 presents a representative set of data for the composites; no corresponding small peaks were observed in the derivative of weight loss data of unfilled epoxy resin. Recall from Fig. 2 that the presence of graphite in composites prevented removal of absorbed water from the specimens. In addition, the composites contained more locked-in water. Consequently, small peaks appeared at around 200 °C for all composites during the thermal degradation test, which correspond to water evaporation. For unfilled epoxy resin, however, the water was almost completely removed at lower temperatures and no water evaporation peak was observed.

4. Conclusions

The study showed that water diffusion in both unfilled epoxy resin and composites followed linear Fickian diffusion behavior. This indirectly indicated that no chemical degradation of epoxy occurred in the composite specimens. It was also seen that incorporation of EG rendered composites more hydrophobic and significantly decreased the maximum water uptake and water diffusivity. Accordingly the composites studied in this work would yield favorable performance for water management in PEM fuel cells. It was seen that composites were dimensionally stable and did not undergo changes in surface appearance and in morphology. The water desorption profile showed that water absorption process was reversible. DSC and TGA data indicated that the composites would be thermally and chemically stable under the PEM fuel cell service conditions. Also long-term hygrothermal exposure would have very little effects on electrical conductivity and mechanical properties of the epoxy composites. Thus, the graphite-based epoxy composites developed in this study would meet most requirements for application as bipolar plates in PEM fuel cells.

Acknowledgements

The authors acknowledge the assistance received from Professor Rex Ramsier in obtaining XPS data. L. Du acknowledges industrial assistantship from Goodyear Tire and Rubber Company.

References

[1] A. Kumar, R.G. Reddy, J. Power Sources 129 (2004) 62–67.
[2] J. Larminie, A. Dicks, Fuel Cell Systems Explained, John Wiley & Sons Ltd., Wiltshire, 2003, pp. 1–108.
[3] J. Huang, D.G. Baird, J.E. McGrath, J. Power Sources 150 (2005) 110–119.
[4] A. Heinzel, F. Mahlendorf, O. Niemzig, C. Kreuz, J. Power Sources 131 (2004) 35–40.
[5] X.G. Li, I. Sabir, Int. J. Hydrogen Energy 30 (2005) 359–371.
[6] W. Vielstich, H.A. Gasteiger, A. Lamm (Eds.), Handbook of Fuel Cells—Fundamentals, Technology and Applications, vol. 3, Fuel Cell Technology and Applications, Wiley & Sons, New York, 2003, pp. 286–293.
[7] J.G. Clulow, F.E. Zappitelli, C.M. Carlstrom, J.I.L. Zemsky, D.N. Busick, M.S. Wilson, Fuel cell technology: opportunities and challenges, in: Topical Conference Proceedings, 2002 AIChE Spring National Meeting, New Orleans, LA, March 10–14, 2002, pp. 417–425.
[8] A.-M. Lafront, E. Ghali, A.T. Morales, Electrochim. Acta 52 (2007) 5076–5085.
[9] H. Tawfik, Y. Hung, D. Mahajan, J. Power Sources 163 (2007) 755–767.
[10] Y. Show, M. Miki, T. Nakamura, Diamond Relat. Mater. 16 (2007) 1159–1161.
[11] Y. Wang, D.O. Northwood, J. Power Sources 163 (2006) 500–508.
[12] S.-H. Wang, J. Peng, W.-B. Lui, J.-S. Zhang, J. Power Sources 162 (2006) 486–491.
[13] I.E. Paulauskas, M.P. Brady, H.M. Meyer III, R.A. Buchanan, L.R. Walker, Corros. Sci. 48 (2006) 3157–3171.
[14] B. Cunningham, D.G. Baird, J. Mater. Chem. 16 (2006) 4358–4388.
[15] J.M. Keith, J.A. King, M.G. Miller, A.M. Tomson, J. Appl. Polym. Sci. 102 (2006) 5456–5462.
[16] F. Barbir, J. Braun, J. Neutzler, J. New Mater. Electrochem. Sys. 2 (1999) 197–200.
[17] S. Gottesfeld, T. Zawodzinski, Adv. Electrochem. Sci. Eng. 5 (1997) 195–301.
[18] E.A. Cho, U.-S. Jeon, H.Y. Ha, S.-A. Hong, I.-H. Oh, J. Power Sources 125 (2004) 178–182.
[19] B. Cunningham, D.G. Baird, J. Power Sources 168 (2007) 418–425.
[20] T.M. Besmann, J.W. Klett, J.J. Henry Jr., E. Lara-Curzio, J. Electrochem. Soc. 147 (2000) 4083–4086.
[21] J.-K. Kuo, C.-K. Chen, J. Power Sources 162 (2006) 207–214.
[22] M.L. Clingerman, E.H. Weber, J.A. King, K.H. Schulz, Polym. Compos. 23 (2002) 911–924.
[23] R. Blunk, F. Zhong, J. Owens, J. Power Sources 159 (2006) 533–542.
[24] V. Meha, J.S. Copper, J. Power Sources 114 (2003) 32–53.
[25] A. Hermann, T. Chaudhuri, P. Spagnol, Int. J. Hydrogen Energy 30 (2005) 1297–1302.
[26] L. Du, S.C. Jana, J. Power Sources 172 (2007) 734–741.
[27] W.S. Chow, A. Abu Bakar, Z.A. Mohd Ishak, J. Appl. Sci. 98 (2005) 780–790.
[28] Y. Wang, T.H. Hahn, Compos. Sci. Technol. 67 (2007) 92–101.
[29] O.D.L. Osa, V. Alvarez, A. Vazquez, J. Compos. Mater. 40 (2006) 2009–2023.
[30] E.E. Shin, R.J. Morgan, J. Zhou, J. Lincoln, R. Jurek, D.B. Curliss, J. Thermoplast. Compos. Mater. 13 (2000) 40–57.
[31] B.N. Yow, U.S. Ishiaku, Z.A. Mohd Ishak, J. Karger-Kocsis, J. Appl. Polym. Sci. 92 (2004) 506–516.
[32] Z.A. Mohd Ishak, U.S. Ishiaku, J. Karger-Kocsis, J. Appl. Polym. Sci. 74 (1999) 2470–2481.
[33] Z.A. Mohd Ishak, B.N. Yow, B.L. Ng, H.P.S.A. Khalil, H.D. Rozman, J. Appl. Polym. Sci. 81 (2001) 742–753.
[34] P.K. Ray, S. Mula, U.K. Mohanty, B.C. Ray, J. Reinf. Plast. Compos. 26 (2007) 519–524.
[35] T. Shimokawa, S. Sanbongi, H. Mizuno, J. Compos. Mater. 36 (2002) 885–895.
[36] L. Bao, A.F. Yee, C.Y.-C. Lee, Polymer 42 (2001) 7327–7333.
[37] J. Jedidi, F. Jacquemin, A. Vautrin, Compos.: Part A 37 (2006) 636–645.
[38] G. Xian, V.M. Karbhari, J. Appl. Polym. Sci. 104 (2007) 1084–1094.
[39] S.R. Patel, S.W. Case, Int. J. Fatigue 24 (2002) 1295–1301.
[40] E.C. Botelho, R.S. Almeida, L.C. Pardini, M.C. Rezende, Int. J. Eng. Sci. 45 (2007) 163–172.
[41] D. Suh, M. Ku, J. Nam, B. Kim, S. Yoon, J. Compos. Mater. 35 (2001) 264–278.
[42] Z.A.M. Ishak, A. Ariffin, R. Senawi, Eur. Polym. J. 37 (2001) 1635–1647.
[43] Y.C. Lin, X. Chen, H.J. Zhang, Z.P. Wang, Mater. Lett. 60 (2006) 2958–2963.
[44] Y. Yu, X. Yang, L. Wang, H. Liu, J. Reinf. Plast. Compos. 25 (2006) 149–160.
[45] E.C. Botelho, L.C. Pardini, M.C. Rezende, Mater. Sci. Eng. A 452/453 (2007) 292–301.
[46] J. Zhou, J.P. Lucas, J. Thermoplast. Compos. Mater. 9 (1996) 316–328.
[47] J. Zhou, J.P. Lucas, Polymer 40 (1999) 5505–5512.
[48] J. Zhou, J.P. Lucas, Polymer 40 (1999) 5513–5522.
[49] J.S. Earl, R.A. Shenol, J. Compos. Mater. 38 (2004) 1345–1365.
[50] M.Y.M. Chiang, M. Fernandez-Garcia, J. Appl. Polym. Sci. 87 (2003) 1436–1444.
[51] M. Lebbai, J. Kim, M.M.F. Yuen, J. Electron. Mater. 32 (2003) 574–582.
[52] A. Pegoretti, A. Penati, Polym. Degrad. Stab. 86 (2004) 233–243.
[53] M.P. Foulc, A. Bergeret, L. Ferry, P. Ienny, A. Crespy, Polym. Degrad. Stab. 89 (2005) 461–470.
[54] P. Blasi, S.S. D'Souza, F. Selmin, P.P. Deluca, J. Control. Release 108 (2005) 1–9.
[55] L. Bao, A.F. Yee, Compos. Sci. Technol. 62 (2002) 2099–2110.
[56] L. Bao, A.F. Yee, Compos. Sci. Technol. 62 (2002) 2111–2119.
[57] L. Bao, A.F. Yee, Polymer 43 (2002) 3987–3997.
[58] M.L. Costa, S.F.M. de Almeida, M.C. Rezende, Mater. Res. 8 (2005) 335–340.
[59] R.M.V. Pavan, V. Saravanan, A.R. Dinesh, Y.J. Rao, S. Srihari, A. Revathi, J. Reinf. Plast. Compos. 20 (2001) 1036–1047.
[60] B.D. Harper, J.M. Rao, v.H. Kenner, C.H. Popelar, J. Electron. Mater. 26 (1997) 798–804.
[61] D. Cornelia, BMI mechanical properties and performance, in: Proceedings of the High Temple Workshop XV, Santa Fe, New Mexico, January 16-19, 1995, 1995, Paper C-1.
[62] D. Cornelia, Long term hygrothermal durability of composites, in: Proceedings of the High Temple Workshop XVI, Orange Beach, Alabama, January 29–February 1, 1996, 1996, Paper W-1.
[63] A. Lerf, H. He, M. Forster, J. Klinowski, J. Phys. Chem. B 102 (1998) 4477–4482.
[64] S. Stankovich, R.D. Piner, S.T. Nguyen, R.S. Ruoff, Carbon 44 (2006) 3342–3347.
[65] H.C. Schniepp, J. Li, M.J. McAllister, H. Sai, M. Herrera-Alonso, D.H. Adamson, R.K. Prud'homme, R. Car, D.A. Saville, I.A. Aksay, J. Phys. Chem. B 110 (2006) 8535–8539.
[66] S. Stankovich, D.A. Dikin, G.H.B. Dommett, K.M. Kohlhaas, E.J. Zimney, E.A. Stach, R.D. Piner, S.T. Nguyen, R.S. Ruoff, Nature 442 (2006) 282–286.
[67] L. Barral, J. Cano, J. Lopez, I. Lopez-Bueno, P. Nogueira, M.J. Abad, C. Ramirez, J. Therm. Anal. Calorim. 60 (2000) 391–399.
[68] A. Apicella, C. Migliaresi, L. Nicolais, L. Laccarino, S. Roccotelli, Composites 14 (1983) 387–392.